World Academy of Science, Engineering and Technology
International Journal of Biomedical and Biological Engineering
Vol:1, No:6, 2007

Automatic Deactivation in Phased Array Probe for Human Prostate Magnetic Resonance Imaging at 1.5T

Fotios N. Vlachos, Anastasios D. Garetsos, Nikolaos K. Uzunoglu, and Efstathios D. Gotsis

***Abstract*—**A four element prototype phased array surface probe has been designed and constructed to improve clinical human prostate spectroscopic data. The probe consists of two pairs of adjacent rectangular coils with an optimum overlap to reduce the mutual inductance. The two pairs are positioned on the anterior and the posterior pelvic region and two couples of varactors at the input of each coil undertake the procedures of tuning and matching. The probe switches off and on automatically during the consecutive phases of the MR experiment with the use of an analog switch that is triggered by a microcontroller. Experimental tests that were carried out resulted in high levels of tuning accuracy. Also, the switching mechanism functions properly for various applied loads and pulse sequence characteristics, producing only 10 μs of latency.

***Keywords*—**Automatic tuning, prostate imaging, phased array, spectroscopy.

I. Introduction

DURING the last ten years there has been much progress in the development of prostate RF coils for the improvement of the signal-to-noise (SNR) ratio and the resolution of the extracting clinical results. Endocavitary [1], [2] and surface coils [3] of different size and shape have been designed and used with some success, but all lack efficiency, robustness or ease of use.

Endorectal and endourethral coils outclass all surface coils in terms of quality of results, because of their close to prostate positioning. A usual clinical method for MR spectroscopy is the combination of surface with internal coils, which provides accurate assessments of prostate cancer [4], [5]. However, the use of internal coils constitutes an interventional method which has always been a displeasing procedure for patients and many physicians avoid whenever it is possible.

Manuscript received July 31, 2007.

F. N. Vlachos is with the Microwaves and Fiber Optics Laboratory, School of Electrical and Computer Engineering,, National Technical University of Athens (NTUA), 9 Iroon Polytechniou, 15773, Zografou, Greece (phone: +306974797500; fax: +302107723557; e-mail: fvlachos@esd.ece.ntua.gr).

A. D. Garetsos is with the Microwaves and Fiber Optics Laboratory, School of Electrical and Computer Engineering,, NTUA, 9 Iroon Polytechniou, 15773, Zografou, Greece (e-mail: a.garetsos@ams-mw.com).

N. K. Uzunoglu is with the Microwaves and Fiber Optics Laboratory, School of Electrical and Computer Engineering,, NTUA, 9 Iroon Polytechniou, 15773, Zografou, Greece (e-mail: nuzu@cc.ece.ntua.gr).

E. D. Gotsis is with the Euromedica Encephalos clinic, 3 Rizariou & Chrisostomou Smirnis, Halandri (e-mail: sgotsis@hol.gr).

Additionally, many attempts have been made in the development of fully autonomic probes for MR Imaging and Spectroscopy. In most of the experimental attempts, emphasis is given on the automatic tuning and matching of the coils in order to enhance its performance and accelerate the initialization procedures of the MR experiment that keep the patient for an extensive period of time in the MRI bore [6], [7].

All automatically tuned and matched coils require being compatible with the pulse sequences used in the MR experiment, which implies detuning of the coils during the RF pulse transmission and re-tuning for the MR signal reception at the Larmor frequency. A series of complex automatic deactivation techniques have been developed and tested in the past [8], which function in parallel with the tuning and detuning procedures but suffer robustness and poor results.

The most common deactivation technique that has been applied in both conventional and experimental non-automatic configurations is the use of PIN diodes at the back-end of the probe [9], [10]. These configurations, however, are totally dependable on the external signals that the MR scanner supplies in order to turn on or off the PIN diode.

In this study, we present a simple and robust prototype phased array surface probe for human prostate imaging designed to bring satisfactory imaging and spectroscopic results without the use of internal coils. The probe is activated and deactivated automatically during the various phases of the MR experiment and is applicable for full clinical use. It does not require the presence of any external signals and is fully functionable with a large variety of RF pulse lengths and powers.

II. Materials and Methods

A. Coil Design and Simulation

The design of the prototype phased array system consists of four rectangular coils. The material used for the construction was copper tape 1 cm wide and 1 mm thick. The use of copper tape decreases the resistance of the coil, thus improving the probe's quality factor Q, because at RF frequencies greater than 1MHz current flows near the surface of the wires (skin effect). The coils are distributed into two pairs of adjacent elements. Each element has dimensions 8 cm × 16 cm, hence

the surface area a pair covers is approximately 14.7 cm × 16 cm. A rule of thumb when considering the dimensions of an MR coil is that the surface area that it covers should have width or length dimensions approximately equal to the depth of the signal sources of interest. The two pairs of coils are inserted into two orthogonal shaped conductor frames made of acetal that are placed on each side of the lower pelvic region (Fig. 1). When a patient is examined the two frames are locked at a fixed distance so that the elements are placed at the center posterior and anterior surface of the pelvic area in order to achieve optimum phased array performance.

The magnetic field and inductance calculations were carried out using the Biot-Savart integral expression. The configuration of the probe was modelled with simulation programming in order to measure the magnetic field's intensity and its drop percentage at the center of the pelvic region with regard to the intensity close to the surface. Computational results showed that the drop percentage does not fall under 7.66% (in the worst case scenario of frames distance 30 cm), when the standard threshold limit is 5% (Fig. 2).

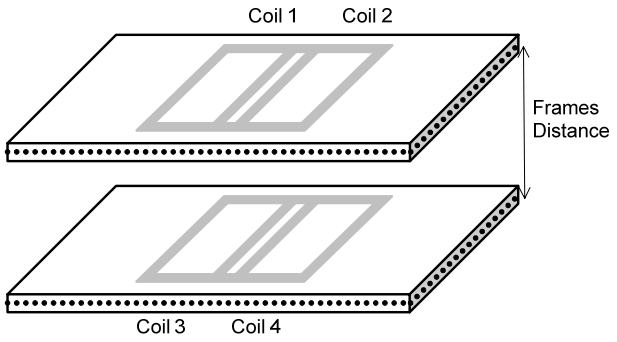

Fig. 1 Phased-array system configuration. Four coils are positioned in pairs inside two conductor frames. The frames distance remains fixed during the examination

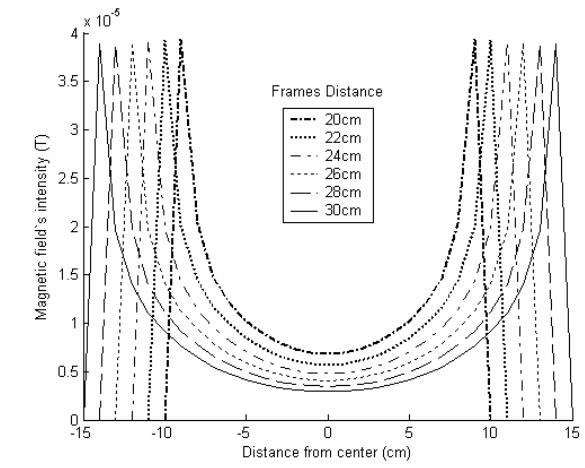

Fig. 2 Theoretical calculations of the magnetic field's intensity for various frames distances (20-30 cm). The measured values correspond to the intensity that is calculated at the line that connects the centers of the parallel frames. The maximum values correspond to the intensity 1 cm away from the frames, close to the test object's surface

The mutual coupling between the phased array coil elements has been taken into consideration in order to eliminate the noise correlation that is produced as a result of the crosstalk between neighbouring circuits [11]. The method that was used for decoupling was the overlapping of the adjacent elements to force the mutual inductance to zero [12]. Theoretical calculations with simulation programming indicated that the distance the adjacent coils should have in order to minimize the mutual inductance is 6.7 cm (Fig. 3). That means that the proper coil overlap is 8-6.7=1.3 cm. Experimental measurements of the S_{21} parameter for various adjacent coils distances with the use of a network analyzer (HP8719D) confirmed the theoretical results.

B. Electronic Methods

Each of the probe's four coils tunes the corresponding load to the Larmor frequency, matches the output impedance to 50 Ohm, protects the MRI scanner from high power pulses and controls the probe's switching behaviour. The electronic components that were used at the front-end of the probe were made of non-magnetic material and the rest of the circuitry was placed on a PCB one wavelength away from the coils. The function of the probe is divided into two phases: deactivation and activation. The components' performance varies from one phase to another, thus in this section we will present an analytical description of the circuit's functionalities and each electronic block's usage during both the deactivation and the activation phase.

In the deactivation phase, the MRI scanner transmits the RF pulses that excite the hydrogen molecules of the test object. During that phase, the electronics of the coil system are protected from the high-power RF pulses with the use of a passive blocking circuit that is placed at the front-end of the coils (Fig. 4A). The circuit is a simple network with two anti-

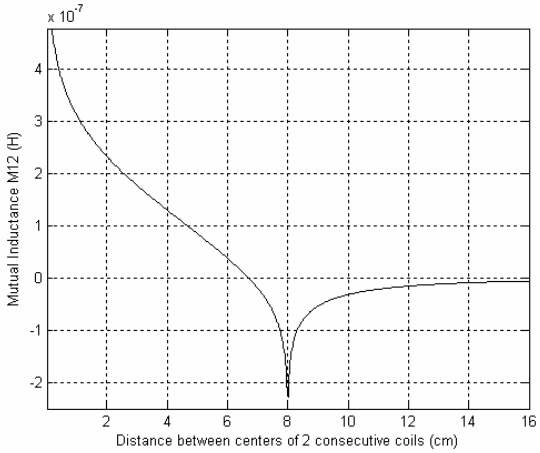

Fig. 3 Theoretical calculation of the optimum overlapping distance between two adjacent rectangular coils with dimensions 8 cm x 16 cm at the Larmor frequency. The minimum value of the mutual inductance M12 is reached at distance 6.7 cm between the centers of the two coils, which implies 1.3 cm overlapping

parallel crossed high-speed diodes (1N4148) that act as a passive switch [13]. Crossed diodes have very high impedance when the signal is small and low impedance when the signal is large. Thus, during the RF pulse transmission the diodes are forward-biased behaving as an effective short circuit, while during the NMR signal reception the diodes are reverse-biased, leaving a fixed and a variable capacitor in parallel to perform a primary tuning of the coils at the Larmor frequency.

A 4:16 balun element at the back-end of the rectangular loop converts the balanced output signal of the coil to 50 Ohm unbalanced. After one wavelength (λ) of 50 Ohm coaxial cable, which is translated into approximately 300 cm for the Larmor frequency (63.87 MHz), a microprocessor serves as the brain of the probe. The circuitry is divided into two operating sections: the matching and the switching circuitry, which collaborate on the tasks of fine-tuning the coil and automatically switching from the deactivation to the activation phase. Those sections will be thoroughly described below.

The matching circuit is a pi-network with two couples of parallel varactor diodes (ZC832) that fine-tune the output impedance of the NMR reception signal (Fig. 4B). The optimum varactors' capacitances are adjusted by two variable DC voltages which are controlled by two trimmer resistors and are amplified by two high-speed low-power precision operational amplifiers (MC34072). The tuning and matching of the probe is done before the NMR experiment with a network analyzer. More specifically, we place the coils on the desired load and then we adjust the values of the DC voltages by varying the capacitance of the trimmers, in order to maximize the output signal.

The transition of the probe from the deactivation to the activation phase is controlled by the switching circuitry. An analog switch (RSW2-25P) is used to block the output of the probe from connecting to the MRI scanner, when the RF pulses are transmitted (Fig. 4D). The switch is triggered by two signals (C1, C2). The microprocessor takes the decision between C1 and C2 using as input the result of a comparator (LM393AD). The comparator compares a pre-defined threshold voltage value with the output DC signal that is produced from the transmitting RF pulses, after they pass through a log detector (AD8307) and two RC low-pass filters (Fig. 4C). When the high power RF pulses are transmitted, then the output DC signal's amplitude is higher than the threshold voltage and the system enters the deactivation phase (C2 signal triggering). Contrariwise, when the output DC signal's amplitude is lower than the amplitude of the

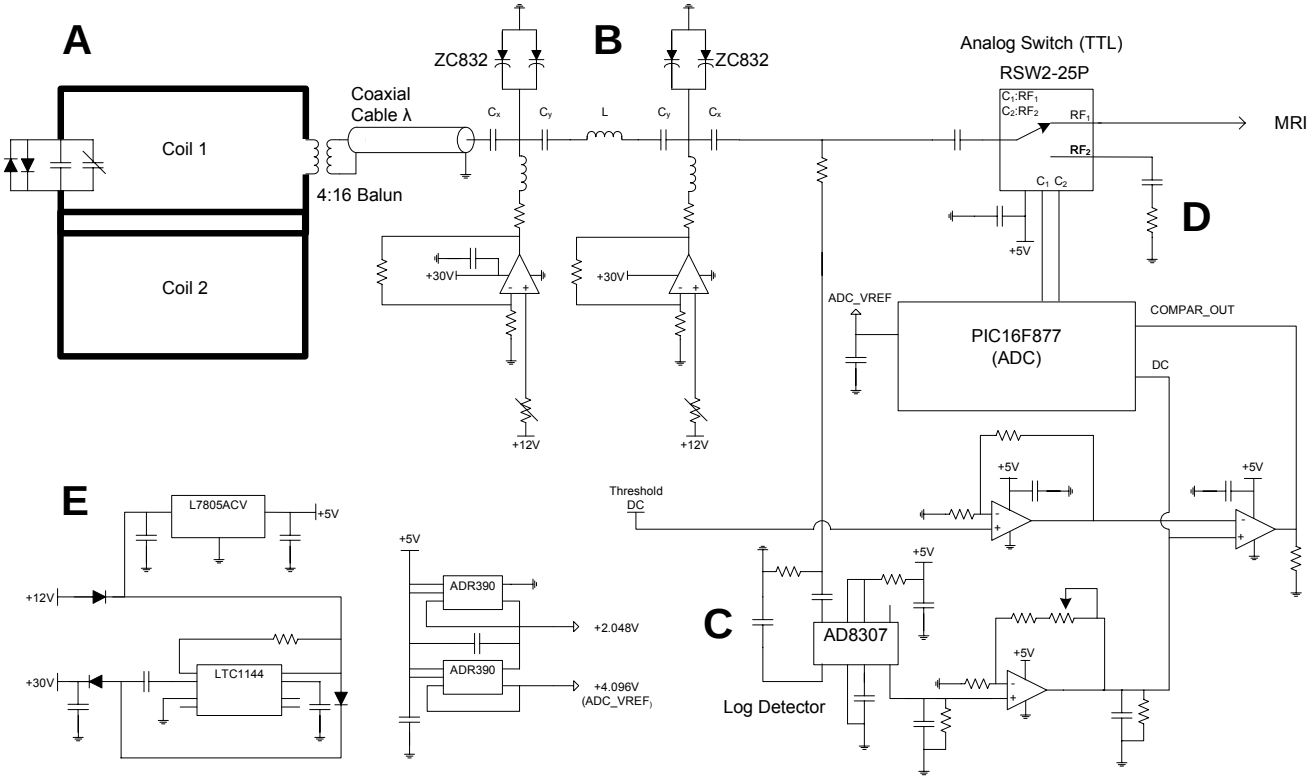

Fig. 4 Receiver coil circuit diagram. The diagram depicts the circuitry of one of the four phased array channels of the probe (A). The tuning/matching circuitries are positioned on four PCBs at λ distance away from the elements. Each circuitry includes three sections (B, C, D) that interact for the tuning and the deactivation of the probe. The tuning section (B) uses two couples of ZC832 varactor diodes in a pi-network to match the output impedance. The feedback section (C) transforms the RF pulses into DC signals fed to the switching section (D), which determines when the probe is in the activation and the deactivation phase and controls an analog switch that connects the probe to the MRI scanner. Additional circuitries on the PCB produce the voltage references for the microprocessor and the rest electronic parts (E)

threshold, it means the system is in the activation phase (C1 signal triggering), receiving low power MR signal from the test object.

The voltage supply of the tuning circuitry is +12V DC. A voltage regulator (L7805ACV) and a voltage converter (LTC1144) transform the battery voltage into +5V and +30V respectively for the feeding of the comparator and the amplifiers. Two precision 2.048V band gap references (ADR390) provide the 4.096V voltage reference for the microprocessor (Fig. 4E).

III. Results

Each element of the probe was tuned and tested using the instrumentation of the laboratory. Initially, after the construction of the probe, both coils from each conductor frame were connected to the network analyzer in order to measure the reflection and transmission coefficients with the S-parameters. Fine-tuning was accomplished with the following procedure: First, we placed the frame on the pelvic region of an average-shaped person in order to tune the coils at 63.87 MHz while they are loaded with the human pelvic area. Afterwards, we varied the non-magnetic capacitor at the front-end of each element and measured the S_{11} and S_{22} parameters. The varactors in the pi-network of the probe's matching circuitry helped achieve high levels of tuning accuracy by varying their DC supplies consecutively. The above procedure was repeated several times with various loads on the frames. Each time, we kept a record of the capacitance and DC values we used for the tuning of the coil and in the end we calculated the average of the recorded values, which we finally applied to the non-magnetic capacitor and the varactors respectively.

The S-parameters that were measured for each load indicated not only the successful tuning accuracy of the coils (S_{ii}), but also the accomplished decoupling (S_{ij}) between the adjacent elements. In Fig. 5C it is shown that the S_{22} parameter drops below -55 dB when the frame is positioned on an average human pelvic region. Moreover, the half-power bandwidth does not exceed the range of 250 KHz, which is the limit for successful tuning in the MR experiment in order to prevent excessive noise admittance. When the coil is on air with no load presence the S_{22} value drops at approximately -30 dB (Fig. 5A). The improvement of the S_{22} parameter between measurements without and with load can be also demonstrated in Fig. 5B and 5D. The imaginary part of S_{22} with load presence produces a sharper zero-crossing at the Larmor frequency compare to that of Imaginary S_{22} without load.

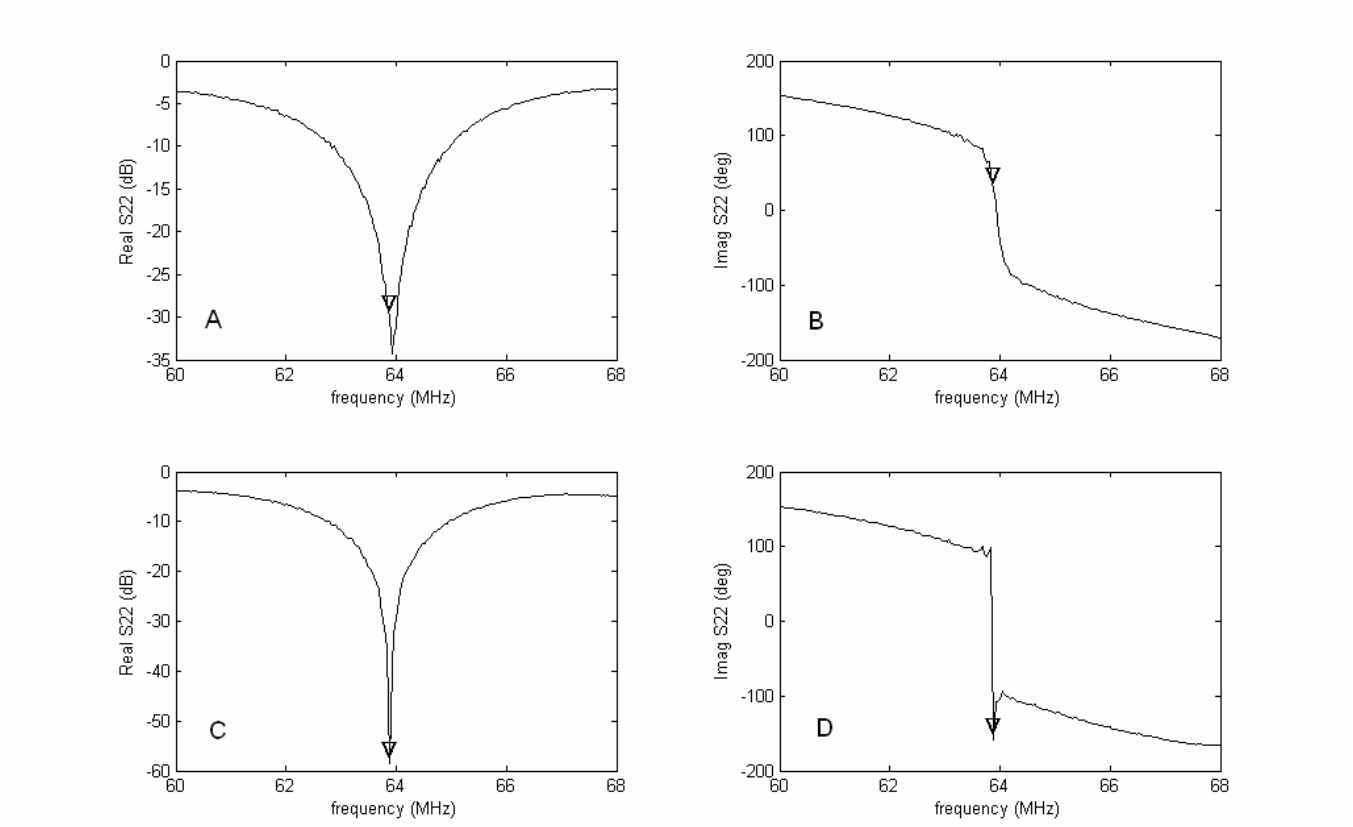

Fig. 5 Quantitative S_{22} measurements. The marker indicates the Larmor frequency 63.87 MHz. (A),(B) Real and Imaginary part of S_{22} when the coil is on air with no load. (C),(D) Real and Imaginary part of S_{22} when the coil is loaded with an average human pelvic region. Note that at 63.87 MHz, S_{22} drops from (A) -30 dB to (C) -55 dB

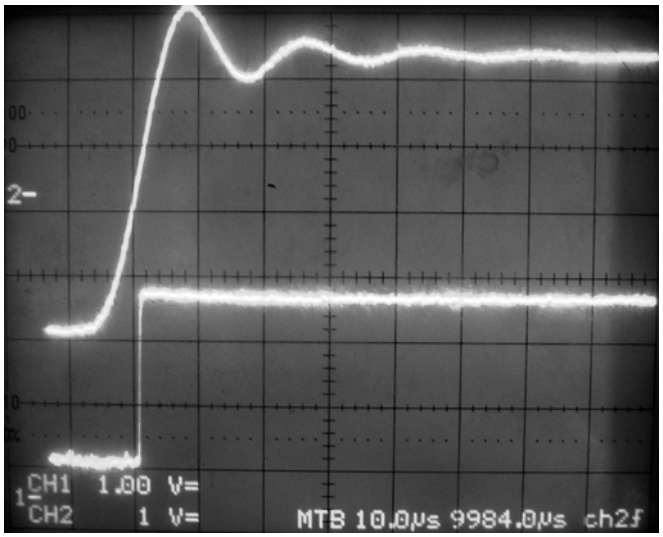

Fig. 6 Log detector's output. The lower line shows the log detector's RF rectification, which produces the DC signal, during the pulse's transmission. The upper line depicts the trigger that generates the RF pulse

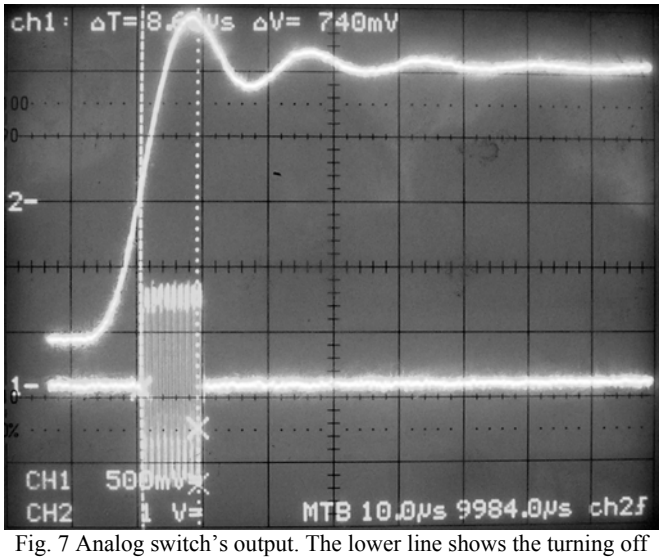

Fig. 7 Analog switch's output. The lower line shows the turning off of the analog switch during RF pulse transmission. 10 μs of RF signal pass through the switch because of the latency caused mainly from the microprocessor. The upper line depicts the trigger that generates the RF pulse

Decoupling between receiver coils was achieved using the overlapping method as it was mentioned before. For the evaluation of the decoupling levels the adjacent elements were both connected to the network analyzer in a full 2-port setting and the transmission coefficients were measured without and with the load of an average human pelvic region. Results showed that the reciprocal S_{21} and S_{12} values fall below -30 dB both with and without load presence.

The correct function of the analog switch was tested in the laboratory using a Signal Generator (HP ESG-4000A) and a Combiscope (FLUKE PM3380B). RF pulses of the same power and length as those transmitted from the MRI system were created in the Signal Generator and were sent through an element of the frame as input. With the Combiscope we first measured the log detector's output and then the output of the analog switch.

The first set of measurements showed that the log detector rectifies the RF pulse into a DC signal almost immediately after the initialization of the signal generator's RF trigger (Fig. 6). The amplitude of that DC signal is then compared with a threshold DC value that is lower than the RF rectified signal and higher than the MR signal to define the phase the experiment is at.

The second set of measurements verified the switching of the analog switch during the transmission of the high power pulses and the MR signal reception respectively (Fig. 7). The presence of an undesired latency of 10 μs in the switching process could be a potential disadvantage, capable of producing artifacts in the clinical data. The latency is caused mainly from the processing delays of the microcontroller that triggers the analog switch. The test was repeated for a variety of pulse lengths and powers in order to assess the comparator's exact threshold DC value and assure that the switch will not be turned off during the reception of the weak MR signal. The experiments showed that the circuitry functioned properly as long as the RF pulses' input power remained over 5 dBm.

IV. Discussion

In this paper we presented a self-controlled phased array system for prostate MR imaging. The design uses rectangular coils of specific size, shape and positioning for optimum performance in the pelvic region. The measurements that were carried out and presented above produced accurate and robust results as far as tuning, matching and decoupling are concerned.

Certain improvements could be applied on the automatic switching mechanism of the circuitry in order to overcome the presence of latency in the function of the analog switch. A way to reduce the latency is to control the switch directly from the DC signal that derives from the comparator's output, bypassing the time-consuming processing of the microcontroller.

Also, a practical problem could potentially appear during the clinical application of the automatic deactivation circuitry in MRI scanners. The probe detunes itself automatically during the RF pulse transmission with the use of the switch and does not require a decoupling signal from the scanner. However, many MRI scanners' protocols run primary tests on the connected probes by sending pulse signals in the opposite direction for software initialization. In that case, the switch would cause compatibility issues and the probe would not be recognized by the MR system.

Our phased array coils focus on the improvement of the SNR in prostate MRI tests and more specifically in MR spectroscopy, where the need for higher spectral resolution is increased. Additionally, the automatic deactivation mechanism that each coil has is able to accurately support the

tuning and detuning of the system and accelerate the initialization procedures.

REFERENCES

[1] D. J. Gilderdale, N. M. DeSouza, G. A. Coutts, M. K. Chui, D. J. Larkman, A. D. Williams, and I. R. Young, "Design and use of internal receiver coils for magnetic resonance imaging," *The British Journal of Radiology*, vol. 72, pp. 1141-1151, 1999.

[2] A. C. Yung, A. Y. Oner, J-M. Serfaty, M. Feneley, X. Yang, and E. Atalar, "Phased-Array MRI of Canine Prostate Using Endorectal and Endourethral Coils," *Magnetic Resonance in Medicine*, vol. 49, pp. 710-715, 2003.

[3] S. M. Wright, and L. L. Wald , "Theory and Application of Array Coils in MR Spectroscopy," *NMR in Biomedicine*, vol. 10, pp. 394-410, 1997.

[4] F. V. Coakley, J. Kurhanewicz, Y. Lu, K. D. Jones, M. G. Swanson, S. D. Chang, P. R. Carroll, and H. H. Hricak, "Prostate Cancer Tumor Volume: Measurement with Endorectal MR and MR Spectroscopic Imaging," *Radiology*, vol. 223, pp. 91-97, 2002.

[5] J. Scheidler, H. Hricak, D. B. Vigneron, K. K. Yu, D. L. Sokolov, L. R. Huang, C. J. Zaloudek, S. J. Nelson, P. R. Carroll, and J. Kurhanewicz, "Prostate Cancer: Localization with Three-dimensional Proton MR Spectroscopic Imaging – Clinicopathologic Study," *Radiology*, vol. 213, pp. 473-480, 1999.

[6] R. Pérez de Alejo, C. Garrido, P. Villa, I. Rodriguez, J. J. Vaquero, J. Ruiz-Cabello, and M. Cortijo, "Automatic Tuning and Matching of a Small Multifrequency Saddle Coil at 4.7T," *Magnetic Resonance in Medicine*, vol. 51, pp. 869-873, 2004.

[7] F. Hwang, and D. I. Hoult, "Automatic Probe Tuning and Matching," *Magnetic Resonance in Medicine*, vol. 39, pp. 214-222, 1998.

[8] R. D. Venook, B. A. Hargreaves, G. E. Gold, S. M. Conolly, and G. C. Scott, "Automatic Tuning of Flexible Interventional RF Receiver Coils," *Magnetic Resonance in Medicine*, vol. 54, pp. 983-993, 2005.

[9] E. A. Barberi, J. S. Gati, B. K. Rutt, and R. S. Menon, "A Transmit-Only/Receive-Only (TORO) RF System for High-Field MRI/MRS Applications," *Magnetic Resonance in Medicine*, vol. 43, pp. 284-289, 2000.

[10] A. C. Yung, A. Y. Oner, J. M. Serfaty, M. Feneley, X. Yang, and E. Atalar, "Phased-Array MRI of Canine Prostate Using Endorectal and Endourethral Coils," *Magnetic Resonance in Medicine*, vol. 49, pp. 710-715, 2003.

[11] G. R. Duensing, H. R. Broker, and J. R. Fitzsimmons, "Maximizing Signal-to-Noise Ratio in the Presence of Coil Coupling," *Journal of Magnetic Resonance Series B*, vol. 111, pp. 230-235, 1996.

[12] P. B. Roemer, W. A. Edelstein, C. E. Hayes, S. P. Souza, and O. M. Mueller, "The NMR Phased Array," *Magnetic Resonance in Medicine*, vol. 16, pp. 192-225, 1990.

[13] X. Zhang, and A. Webb, "Design of a Four-Coil Surface Array for in Vivo Magnetic Resonance Microscopy at 600 MHz," *Concepts in Magnetic Resonance Part B*, vol. 24B(1), pp. 6-14, 2005.